Jpn. J. Appl. Phys. Vol. 38 (1999) pp. 3809–3812
Part 1, No. 6B, June 1999

Calculations of Scanning Tunneling Microscopic Images of Benzene on Pt(111) and Pd(111), and Thiophene on Pd(111)

Don Norimi FUTABA*1 and Shirley CHIANG*2

Department of Physics, University of California, Davis, California 95616, U.S.A.

(Received March 8, 1999; accepted for publication March 18, 1999)

We use a computational method, based on extended Hückel molecular orbital theory, for calculating the scanning tunneling microscope (STM) images of benzene on Pt(111), benzene on Pd(111), and thiophene on Pd(111). For each case, we calculated images for both isolated and chemisorbed molecules. From binding energy calculations, the low energy geometries for the three binding sites were determined. The calculated images for benzene on Pt(111) agreed well with previously published experimental and theoretical results. We found many similarities between the calculated images of benzene on Pt(111) and on Pd(111). Calculated images of adsorbed thiophene showed marked similarities with the previously calculated images of furan and pyrrole.

KEYWORDS: STM, scanning tunneling microscope, microscopy, Hückel, palladium, Pd(111), platinum, Pt(111), benzene, thiophene

1. Introduction

In the study of surface chemistry, there lies a great importance in the recognition of various molecular species on a surface. The scanning tunneling microscope is a tool for identifying such differences, but interpreting those images is often unclear. The method of predicting scanning tunneling microscope images, based on extended Hückel molecular orbital theory (EHT), gives the ability to predict particular surface features of given organic adsorbates, and in some cases, preferred binding sites and orientations.[1–3] Although simple and crude when compared with *ab initio* calculations, this simple cluster calculation requires little time and effort in providing initial insight into systems of adsorbed organic molecules on metals.

Because it has been extensively studied, the benzene on Pt(111) system is excellent for comparing the EHT calculations to experimental and theoretical results. In addition, it acts as a stepping stone for our studies of benzene on Pd(111), both theoretically and experimentally. We also used EHT to calculate thiophene on Pd(111) in preparation for variable temperature scanning tunneling microscope (STM) studies of the decomposition of furan, pyrrole, and thiophene on Pd(111). We are motivated by our desire to understand both the use of late transition metals as promoters to remove the heteroatoms from the molecule and the relationship between the surface structure and the surface reactivity.

2. Method

Though limited to organic molecules, a method for predicting STM images based on EHT has been successful in reproducing the detailed internal structures of such carbonring structures as naphthalene, azulene, monomethylazulene, dimethylazulene, and trimethylazulene on Pt(111).[1–3]

The EHT calculation can be simply summarized into two steps: 1) Calculate the preferred molecule-cluster separation for each configuration by plotting the binding energy as a function of molecule-cluster separation; 2) Compute and plot 15 Å × 15 Å images for both occupied and unoccupied states which correspond experimentally to negative and positive sample bias settings.

From the Tersoff-Hamann theory of operation of the STM,[4] the STM image can be interpreted as a two-dimensional map of the surface local density of states (LDOS) evaluated at the Fermi level at the height of the tip. Thus, we use EHT to calculate the energy levels of the system of interest and then evaluate the LDOS for different heights above the molecule at the Fermi level. Varying tip heights in the calculation corresponds to varying the resolution of the STM. An energy integration is performed to include all energy states contributing to the tunneling as governed by the sample bias and to include molecular character related to the hybridization with metal orbitals near the Fermi level, which is not only found in the highest occupied molecular orbital (HOMO) and lowest unoccupied molecular orbital (LUMO).

These programs have been successfully ported from an IBM mainframe computer to a 150 MHz Pentium-based PC. In our study the Pt and Pd metal clusters consisted of a single hexagonal layer of ∼20 atoms. Computation of the energy eigenvalues took approximately 2–5 minutes. Another 2–5 minutes were needed to generate both occupied and unoccupied state images.

Hückel parameters for Pt and Pd were taken from the literature and are in refs. 1 and 3, respectively.

3. Results and Discussion

3.1 Benzene on Pt(111)

For each of the two orientations on the three high-symmetry binding sites, we performed the operations described in the method section. Figure 1 schematically illustrates the various binding sites and orientations of the benzene molecule on the metal surface. Within the EHT calculations, we found that for the on-top site, the 30° orientation was preferred. On the bridge site, the 0° oriented molecule was preferred, while on the 3-fold hollow site, the 30° oriented molecule was favored. Figures 2(b), 2(d) and 2(f) show the three distinctive shapes found, corresponding to a volcano, three bumps, and a single bump as previously seen experimentally.[6] Figure 2 contains calculated images which strongly exhibit the three distinctive shapes for this system.

The surface features associated with each binding site differed only slightly from previous theoretical work by Sautet *et al*.[5] For example, in the case of the on-top site, while both

*1E-mail address: dfutaba@landau.ucdavis.edu
*2E-mail address: chiang@physics.ucdavis.edu

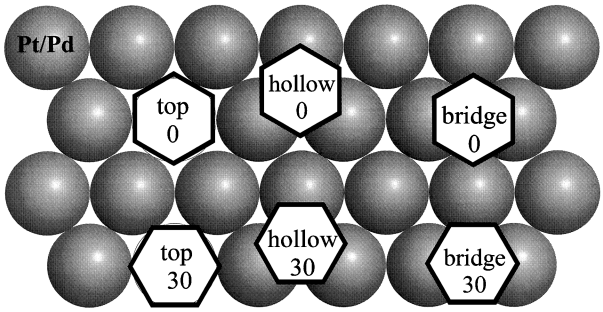

Fig. 1. Schematic diagrams of benzene geometry on the Pt(111) and Pd(111) clusters.

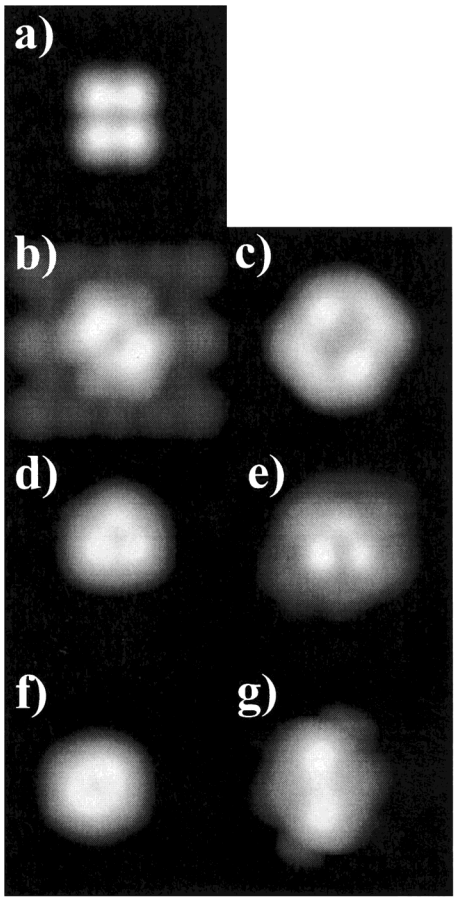

Fig. 2. Calculated images of benzene for the isolated molecule and adsorbed onto metal surfaces. (a) LUMO; unoccupied states image of benzene adsorbed onto the on-top site (b) at 30° on Pt(111) and (c) at 0° on Pd(111); unoccupied states image on the 3-fold hollow site (d) at 0° Pt(111) and (e) at 0° on Pd(111); unoccupied states image on the bridge site (f) at 0° on Pt(111) and (g) at 0° on Pd(111).

orientations demonstrated a six-fold symmetry and a centered dimple, as Sautet found, the 0° orientation showed a substantially weaker dimple seen only when the LDOS was evaluated at a smaller separation. For the 3-fold hollow site, we found the 0° configuration to demonstrate a stronger 3-fold symmetry while the 30° arrangement showed more of a six-fold symmetry. In contrast, although Sautet found differences in the prominence of features between the two orientations of benzene on the 3-fold hollow site, both exhibited 3-fold symmetry. For the bridge site, we observed a single bump in the unoccupied states image, but found a pronounced two lobe feature in the occupied states image which is discussed further in the next section for benzene on Pd(111). From both experimental results by Eigler *et al.*[6] and the aforementioned theoretical results by Sautet *et al.*,[5] the bridge site produced a single bump feature. The features of the calculated images themselves clearly showed the same symmetries seen in experimental STM data.

3.2 Benzene on Pd(111)

We performed the same type of calculations for benzene on Pd(111). The schematic orientations of benzene on Pd are shown in Fig. 1. Since Pd has the identical crystal structure, an almost identical lattice constant, and is from the same group of the periodic table as Pt, the calculated images of the adsorbed benzene on Pd show the same three distinctive shapes which characterized the adsorbed benzene on Pt. Also, benzene on Pd exhibited the same energetic preferences as the Pt case. We found that the on-top site 30° orientation, the 3-fold hollow site 30° orientation, and the bridge site 0° orientation were the preferred geometries on their respective site, with the on-top site being the most favorable.

One difference, however, is seen in the relatively larger size of the on-top site image for palladium. Figures 2(c), 2(e) and 2(g) show the characteristic features we hope to resolve experimentally.

Another difference is the two lobe feature we found on the bridge site. However, the experimental images for the bridge site may be quite different from those calculated here if the sample-tip effects from calculations by Sautet *et al.*[5] for benzene on Pt(111) apply here as well. Experimentally, benzene on a Pt(111) bridge site demonstrated a single bump feature,[6] which was attributed to interference between the tunneling current through the molecule and directly from the metal. Apparently, the interference was constructive in the center and destructive outside the carbon ring, resulting in convolving a two peak image to a single peak. The other binding sites showed these effects to a much lesser degree. Thus, for the EHT calculations shown here, our assumption that the images are a result from current through the molecule only is probably reasonable for the on-top and 3-fold hollow sites.

3.3 Thiophene on Pd(111)

Figure 3(a) is a schematic diagram of thiophene, together with the simliar molecules furan and pyrrole. Figure 3(b) shows the resultant low energy binding sites and orientations from the binding energy calculations for thiophene on Pd(111). As determined from the binding energy plots, Fig. 4, the computations show a slight preference for the 0° oriented thiophene on the on-top site. Thiophene on 3-fold hollow sites slightly favors the 0° orientation. Thiophene on the bridge site shows no clear preference between orientations. Because the calculated images for both of the orientations on the bridge site are quite similar, we only present images for the 90° oriented case. Moreover, the differences between the two are so subtle that we do not expect to be able to differentiate between the two in an experiment.

Figure 5 is a set of the predicted images corresponding to the configurations for thiophene on a Pd(111) cluster. The two columns are images for the same binding site but at different tip heights. We can extract more detailed structural information from images with the LDOS calculated closer to

the molecular plane, which correspond to higher resolution STM images with more molecular detail, as expected. Figures 5(a) and 5(b) are the LUMO's for the isolated molecule at two different heights above the surface. Not surprisingly, because of the great similarity of thiophene to furan and pyrrole, the LUMO shows a strong similarity to that of furan and pyrrole.[3] Just as with the case of furan, we speculate that the strong electron density along the carbon backbone is due to the dipole moment of thiophene. In the on-top site unoccupied state images (Figs. 5(c)–5(d)), we see how the cluster affects the image of thiophene. Based on its location and the fact that sulfur is more electronegative than carbon, the relatively dim feature in Fig. 5(c) is the sulfur atom itself which is centered below the bright carbon backbone. In contrast, in the occupied states images, the sulfur heteroatom appears brighter than the carbon backbone. In addition, because of the small molecule cluster separation, as seen in Fig. 4, we are able to resolve both the molecule and metal cluster in Fig. 5(d). With the exception of the relative intensity, the 3-fold hollow site images in Figs. 5(e)–5(f) show similari-

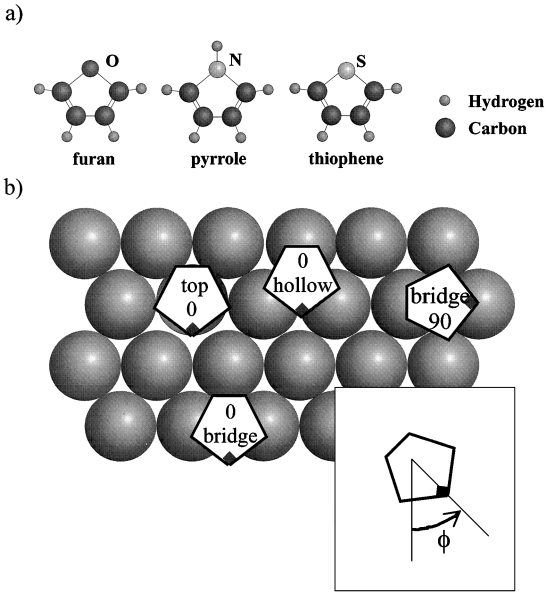

Fig. 3. (a) Schematic diagrams of furan, pyrrole, and thiophene. (b) The low energy adsorption geometries of thiophene on Pd(111) for the high symmetry binding sites: on-top, 3-fold hollow, and bridge sites. The numerals indicate the rotation angle in degrees, ϕ, of the heteroatom as shown in the inset.

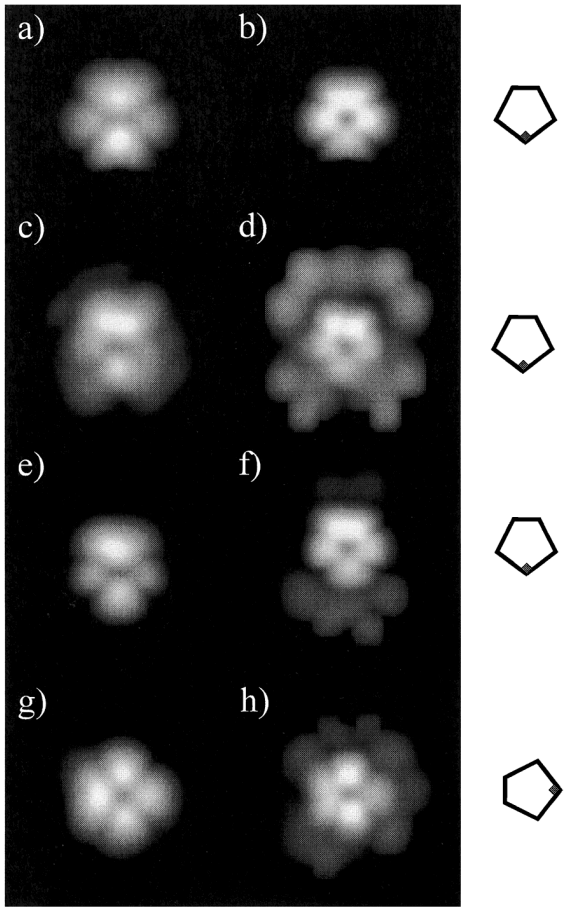

Fig. 5. Thiophene on Pd(111). Schematic drawings of thiophene are shown to clarify the orientation for each binding site. LUMO for isolated thiophene rotated 0° at (a) 2 Å and at (b) 0.5 Å above the molecular plane. Unoccupied states for on-top site rotated 0° at (c) 2 Å and at (d) 0.5 Å above the molecular plane; 3-fold hollow site rotated 0° at (e) 2 Å and at (f) 0.5 Å above the molecular plane; bridge site rotated 90° at (g) 2 Å and at (h) 0.5 Å above the molecular plane.

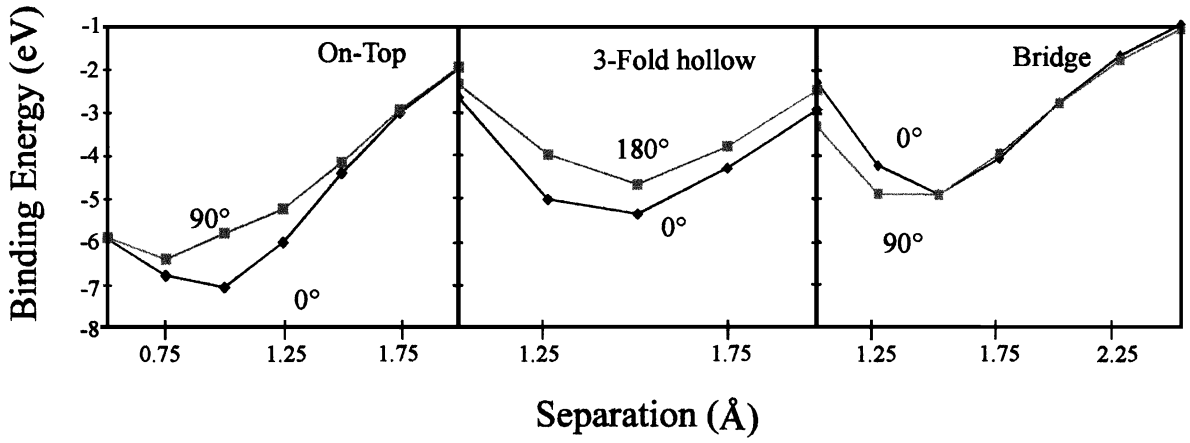

Fig. 4. Binding energy curves for thiophene adsorbed onto Pd(111). Three different binding sites were investigated: on-top, 3-fold hollow, and bridge. Different symbols indicate the azimuthal orientation of the molecule with respect to the lattice, as indicated in Fig. 3(b).

ties in symmetry to the on-top site images. We suspect that this increased intensity is a result of the higher coordination with substrate atoms resulting in an intensified local density of states. Features in the bridge site images (Figure 5(g)–5(h)) show a admixture of features of the LUMO and the other two sites. Again, the spatial imbalance in the LDOS intensity of the 90° bridge site (from left to right) is a result of the dipole moment of the thiophene.

We might expect thiophene to adsorb with the sulfur heteroatom bonded to the metal surface, and with the molecular plane at a tilt or normal to the metal surface, as suggested by Ormerod *et al.*[7] for furan. Given these circumstances, we have performed calculations for furan vertically oriented on the palladium cluster. A pair of carbon atoms was relatively high above the surface and not likely to hybridize with surface atoms. The resultant image was characterized by two carbon-originated lobes.

4. Conclusions

Predicted STM images were presented for benzene on Pt(111) and Pd(111), and thiophene on Pd(111), using EHT as the basis for the calculations. We expect the 30° on-top site to be the most favorable one for benzene on both Pt and Pd, and the bridge site to be the most probable binding site for thiophene on Pd. However, all three binding sites may be possible for low temperature physisorbed or chemisorbed molecules, as for benzene on Pt(111) at 4 K.[6] Because of the characteristic shapes for benzene adsorbed on Pd, we expect to be able to differentiate between benzene on the three binding sites. Conversely, for thiophene on Pd, because of the relatively subtle differences between surface features for the various binding sites, we do not expect to be able to differentiate between molecules adsorbed on different binding sites. In addition, because of the similarity of the features in the predicted images with those of furan and pyrrole, we would not expect to be able to distinguish between these three molecules adsorbed simultaneously.

Acknowledgments

We acknowledge Quantum Chemistry Program Exchange (QCPE) for the program FORTICON 8. We also gratefully thank V. M. Hallmark and B. Lau for their helpful discussions. This work was supported by the National Science Foundation under Grant No. CHE-95-20366 and by the Campus Laboratory Collaborations Program of the University of California.

1) V. M. Hallmark and S. Chiang: Surf. Sci. **329** (1995) 255.
2) V. M. Hallmark, S. Chiang, K.-P. Meinhardt and K. Hafner: Phys. Rev. Lett. **70** (1993) 3740.
3) D. N. Futaba and S. Chiang: J. Vac. Sci. Technol. A **15** (1997) 1295.
4) J. Tersoff and D. R. Hamann: Phys. Rev. Lett. **50** (1983) 1998.
5) P. Sautet and M.-L. Bocquet: Phys. Rev B **53** (1996) 4910.
6) P. S. Weiss and D. M. Eigler: Phys. Rev. Lett. **71** (1993) 3139.
7) R. M. Ormerod, C. J. Baddeley, C. Hardacre and R. M. Lambert: Surf. Sci. **360** (1996) 1295.